University of Applied Sciences

HOCHSCHULE
EMDEN·LEER

Fachbereich Seefahrt

Jürgen Göken, Sarah Fayed

A Report on Different Vibration Analyses Based on Acoustic and Mechanical Measurements

Schriftenreihe der Hochschule Emden/Leer, Band 23

Jürgen Göken, Sarah Fayed

A Report on Different Vibration Analyses Based on Acoustic and Mechanical Measurements

Hochschule Emden/Leer
Emden 2017

Schriftenreihe der Hochschule Emden/Leer, Band 23

Verlag: Hochschule Emden/Leer
Druckerei: VON DER SEE, Emden
Buchbinderei: VON DER SEE, Emden

Hochschule Emden/Leer
Constantiaplatz 4
26723 Emden
E-Mail: bibliothek.emden@hs-emden-leer.de

ISBN: 978-3-944262-13-0

University of Applied Sciences Emden/Leer
Faculty of Maritime Studies

- Laboratory of Materials Physics -
Head of laboratory: Prof. Dr. rer. nat. habil. Jürgen Göken
Scientific assistant: M.Sc. Sarah Fayed

A Report on Different Vibration Analyses Based on Acoustic and Mechanical Measurements

Contact

Prof. Dr. rer. nat. habil. Jürgen Göken
University of Applied Sciences Emden/Leer
Faculty of Maritime Studies
- Laboratory of Materials Physics -
Bergmannstr. 36
26789 Leer, Germany
E-mail: juergen.goeken@hs-emden-leer.de
Phone: 0049-(0)491-92817-5037

Research Topics:

1. Investigation of strain dependent damping of the titanium alloy Ti-10V-2Fe-3Al at room temperature

Lightweight designs offer a major contribution regarding reduced fuel consumption in several transportation fields, e.g. shipping sector, and thus, reduced CO_2 emissions. An effective way to minimise the weight without major changes in the design is the substitution of construction materials with high specific density like steels by lighter titanium alloys [1], [2] with simultaneous maintaining of the strength. Especially in the marine industry, titanium is a suitable construction material due to its low density (roughly half the weight of steel, nickel and copper alloys), its high strength-to density ratio, its high temperature resistance (up to 600 °C) and its remarkable corrosion/erosion resistance. However, the integration of titanium materials in mass production is still low, due to their complex ore processing and poor workability. Therefore, much of the titanium research still focuses on the improvement of its mechanical properties aiming at the optimisation of its workability.

Experimental details

In this investigation, three thermo-mechanically processed specimens of the titanium alloy Ti-10V-2Fe-3Al (shortly, Ti-10-2-3) in a sequence of hot forging and varied conditions of solution treatment and subsequent ageing, were used for studying the vibration behaviour of the material with the help of non-destructive, contact-free acoustic measurements. The variation in the cooling manner of the specimens aimed at producing an obvious difference in the final microstructure, and thus a possibly considerable difference in the damping behaviour of the material. The first Ti-10-2-3 sample was hammer-forged and cooled in air, the second one was hammer-forged and quenched in water and the third one was hammer-forged, quenched in water and aged (520 °C for 2 hours). More details about the processing conditions of the specimens are found in Ref. [3]. The specimens were cut to bending beams of 120 mm length (bending length: about 88 mm), 10 mm width and 2 mm thickness.
The measurements were carried out with the help of a highly sensitive acoustic probe (Microflown™ probe, Microflown Technologies, NL), which was able to accurately measure the sound pressure.
Figure 1 shows a sketch of the experimental set-up used for the acoustic measurements. It consisted of a crank which was attached to a roller on which a tooth was mounted. When the roller was rotated manually the tooth touched the free end of a bending beam and pressed the beam down to a predetermined deflection. Subsequently, the sample performed a freely decaying oscillation after the tooth had passed the free end of the bending beam. The resulting time-dependent sound pressure data values were digitally recorded by a two-channel signal conditioner at a sampling rate of 5 kHz and then transferred to the computer. 25 successive measurements at 5 different flexural vibration amplitudes (different sample deflections) were performed

on each Ti-10-2-3 sample. These measurements served on the one hand for the investigation of the relationship between the bending deflections of the samples and the resulting sound pressure values, and on the other hand, for studying the damping behaviour of different Ti-10-2-3 samples as a function of the strain.

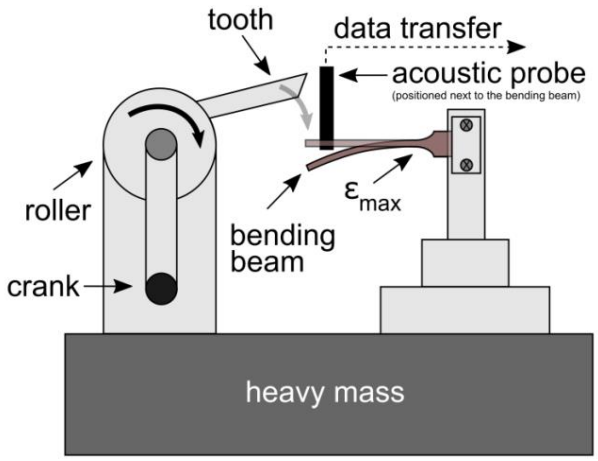

Figure 1: **Experimental set-up of the applied acoustic measurements.**

Acoustic output

Due to the set-up's vibration, which occurs when the vibration energy of the sample is transferred to the whole set-up and also due to other existing residual effects of the apparatus damping, adequate data processing was necessary to obtain a relatively denoised sound pressure signal of the excited sample. For example, the background signal accompanying each of the vibration measurements had to be recorded and eliminated from the total output signal.

A correlation between the maximum values of the sound pressure amplitudes S_n (n = *0,1,2,…*) received by the acoustic probe and the corresponding sample deflection z'_n could be determined by means of the applied measurements at 5 different flexural vibration amplitudes. The results were linearly fitted and plotted in Figure 2.

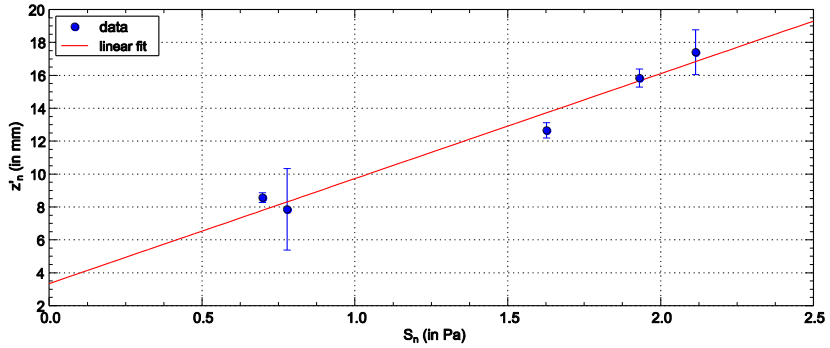

Figure 2: **Correlation between the maximum values of the sound pressure amplitudes S_n and the corresponding sample deflection z'_n.**

The acoustic measurements verified that the maxima of the decaying sound pressure can, in a good approximation, directly be attributed to the corresponding temporal decrease of the sample deflections (amplitudes of flexural vibration).

Results and discussion

The micrographs representing the microstructural changes due to the mentioned processing methods are described in detail in Ref. [3].
In order to analyse the variation in the decay behaviour of the output signal that indicate microstructural differences, the maxima (peak values) of the time-dependent acoustic signal were determined with the help of a self-written program in LabVIEW from National Instruments™ using a parabolic curve fit. An exponential decay of the obtained peak values was then applied on the decaying output signal. The temporal decay of the peak values $S(t)$ can be written as

$$S(t) = S_0 e^{-\beta t} + b, \tag{1}$$

where S_o is the initial sound pressure amplitude, $S(t)$ is the time-dependent sound pressure amplitude and b is a constant offset. The damping constant β could be determined from the decay of the signal's envelope curves for the three investigated Ti-10-2-3 samples. The corresponding damping constants β from Eq. (1) for the three Ti-10-2-3 samples were: β = 16.6 s^{-1} for the as-forged and cooled in air sample, β = 36.8 s^{-1} for the as-forged and quenched in water sample, and β = 8.6 s^{-1} for the as-forged, quenched in water and aged sample. The variation in the β values emphasise the difference in the specimens' microstructures, which lead to significant changes in the strain dependent damping. The current maximum strain value $\varepsilon_{max,n}$ can be determined from the current sound pressure amplitude $S_n(t)$ as:

$$\varepsilon_{\mathrm{max,n}} = \frac{3a}{2l^2} c S_{\mathrm{n}}(t), \tag{2}$$

where a and l represent the thickness and the length of the sample, respectively, and c is the slope of the linearly fitted curve in Figure 2. The logarithmic decrement method had been used to determine the damping of the investigated samples in time domain. It is assumed that the temporal decay of the sound pressure amplitudes corresponds to the temporal decay of the amplitudes of the flexural vibration. Thus, the material damping could be received by measurements of $S_n(t)$. Taking the drop of the sound pressure amplitude in k successive cycles into consideration, the logarithmic decrement δ is obtained from

$$\delta = \frac{1}{k} \ln\left(\frac{S_{\mathrm{n}}(t)}{S_{\mathrm{n+k}}(t)} \right), \tag{3}$$

where $S_n(t)$ is the sound pressure amplitude at the time nT (T: cycle time) and $S_{n+k}(t)$ is the drop of amplitude in k successive cycles later at the time $(n+k)t$ in free decay vibration [4]. Due to the dependence of the apparatus damping δ_a at very low ε_{max} on individual acoustic conditions, the data of a very stiff reference sample and also those of the titanium specimens were used to calculate an average apparatus damping $\delta_a \approx$

$12x10^{-3}$. This value was subtracted from the calculated logarithmic decrement for each of the three Ti-10-2-3 samples. Owing to the presence of energy dissipation in air in addition to the energy dissipation in the solid, a higher material damping than expected was achieved. An approximation of the resulting data were applied by dividing the experimentally obtained data by the value 100 (Figure 3), which relates to earlier own studies on the stiff reference sample's damping behaviour.

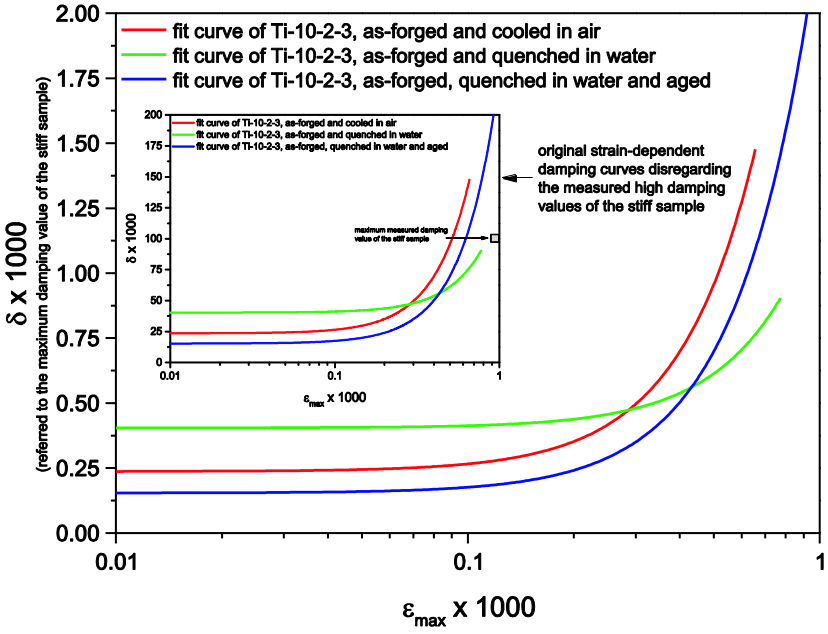

Figure 3: **Fitted strain-dependent damping curves of Ti-10-2-3 samples after different thermal treatment procedures.**

All curves showed a strain-independent (δ_0) and a strain-dependent part (δ_h). It is obvious that the sample which was hammer-forged and quenched in water tended to have the highest damping value, as approximately expected from the damping constants β or the envelope fit curves. The corresponding microstructure [3] was characterised by a high amount of precipitates. This means a flagrant impoverishment of atoms in the matrix which has a significant impact on the material damping [5].

It can be assumed that dislocation damping is the main source of the experimentally received curve progression. The damping mechanism is explained by the Koehler-Granato-Lücke (K-G-L) vibrating string model proposed by Koehler [6] and developed further by Granato and Lücke [7], Figure 4. Experimental findings of Bleasdale and Bacon [8] approved this assumption and proposed that high strains increase the mobile dislocation density and thus increase the damping at lower strains. In case of precipitation development, the distance between the strong pinning points of the matrix becomes larger. As a consequence, the dislocation segment is more moveable which leads to a higher damping. It could be observed that subsequent ageing after water quenching resulted in a distinct reduction of damping. This can be attributed to a re-pinning of the dislocations because some precipitations were dissolved again. Moreover, a higher maximum strain amplitude for a break-away of dislocations from pinning points for the water-cooled sample was detected. This gives

an indication that the dislocations are less movable due to the rapid cooling which can be traced to higher stresses in the material.

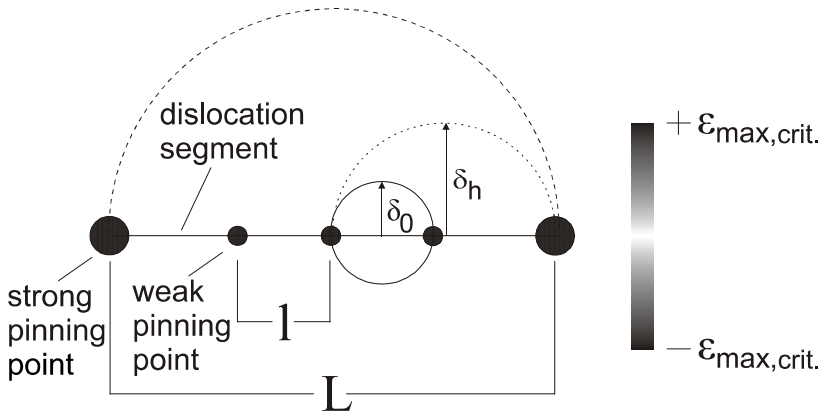

Figure 4: **Pinning and bowing out of a dislocation segment according to the K-G-L model. l : dislocation segment between weak pinning points, L : dislocation segment between strong pinning points.**

Conclusions

The Ti-10V-2Fe-3Al alloy (Ti-10-2-3), which is characterised by its high tensile strength and high resistance against creep, underwent a high strain rate deformation as an alternative for isothermal or cost-intensive hot die forging. Since the cooling process has a strong influence on the microstructural development, especially by the evolution of precipitates, structure-sensitive damping measurements were carried out on different Ti-10-2-3 samples (hammer-forged and cooled in air; hammer-forged and quenched in water; hammer-forged, quenched in water and aged (520 °C for 2 hours)) using an acoustic set-up.

It was found that the decaying sound pressure can, in a good approximation, directly be attributed to the corresponding temporal decrease of the sample deflections. Based on this correlation, the logarithmic decrement method has been used to measure the material damping as a function of the maximum strain amplitude of the sample. The obtained results were in correlation with the sequence of the material damping of Ti-10-2-3 samples as received from the slope of the decay curves of sound pressure measurements.

The curve progression of the strain-dependent damping curves was explained in the framework of the Koehler-Granato-Lücke (K-G-L) string model where dislocations are pinned by strong and weak pinning points. When precipitation takes place, the matrix becomes depleted in atoms which leads to a stronger bowing out of dislocation segments and, thus, to a higher material damping. This could be observed for the Ti-10-2-3 sample which was hammer-forged and quenched in water whereas the amount of precipitations was expected to be reduced by ageing because the material damping was lower. The strain dependence of the damping of the Ti-specimen which was hammer-forged and cooled in air allows the conclusion that the dislocations are pinned

more strongly which can be due to high stresses in the material by this cooling procedure.

2. Acoustic measurements of sound distribution on different organ pipes and on a piano sounding board using different acoustic detection systems

The aim of these investigations was to localise the sound emission and thus accomplish a picture of the acoustic radiation behaviour on the walls of different musical instruments. The manufactures assume that the design and specific adjustments on their instruments have great influence on a harmonic sound development. This assumption had to be scientifically approved. To localise the sound emission, different acoustic measuring instruments were used. In a first experiment, different organ pipes were placed in the centre of a 3D-microphone array with the goal to create a 3D-beamforming picture showing the specific sound field of the pipes. A second experiment involved the measurement of a piano soundboard which is either tuned with or without special weights. In order to localise the proper position for the weights, the measurement was carried out with a spiral array and a mobile handheld array which gives a live translation of the recorded data for immediate comparison.

- Acoustic measurements of different organ pipes

Experimental details

The acoustic measurements on different organ pipes were applied with the help of a 3D beamforming method. The measurement object is positioned in a cubic microphone array (80 x 80 x 80 cm^3), where each of 4 array walls is equipped with 12 MEMS microphones of 24 bit resolution, a sampling rate of 48 kHz and a frequency range of 20 Hz to 20 KHz. Besides the microphone arrangements, a digital camera was mounted in the middle of one of the array walls, and thereby provide an acoustic camera system that synchronously record the incident sounds on the microphones and display the position and the intensity of sound colour-coded on the computer's screen. The three-dimensional location of each microphone and that of the camera in the cubic array were recorded in the associated software, where also other technical adjustments were required to establish a correct coordination between the acoustic setup and the software.

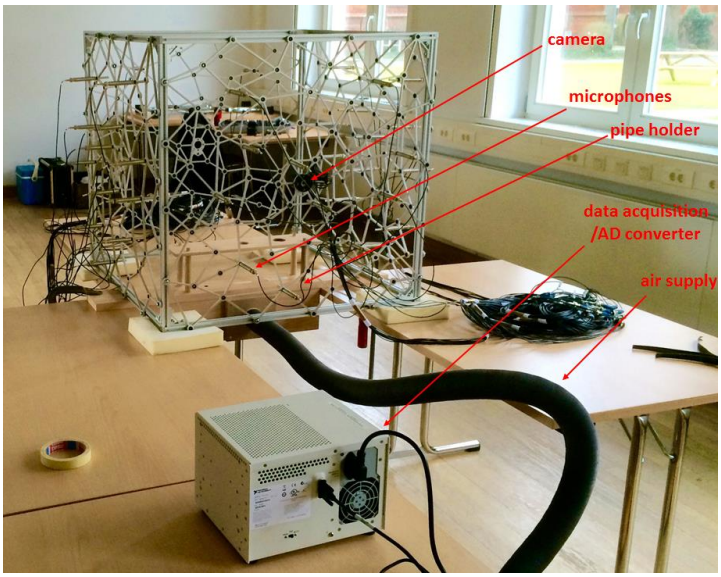

Figure 5: **Experimental setup of the acoustic measurements on organ pipes using a 3D microphone array and a mounted digital camera.**

The experimental setup (Figure 5) consisted of: a 3D array with 48 mounted microphones and a digital camera, an organ pipe holder with different openings for different sized pipes, an air compressor which was used to activate the oscillation of the air column inside the attached pipe and afford sound production, and a data acquisition system with a PC. A measurement had a length of 10 seconds, and the measurements have been recorded in a frequency range of 200 to 2000 Hz. Different metal pipes (thick- and thin-walled high-alloyed, thick- and thin-walled low-alloyed) and different wooden pipes (thin-walled hardwood, thick- and thin-walled softwood) and a reed organ pipe have been acoustically measured.

Results and discussion

The following figures demonstrate some of the resulting 3D colour-coded beamforming measurements of the organ pipes, showing sound emission behaviours that to some extent differ with respect to wall thicknesses and sizes, and obviously with respect to materials and shapes.

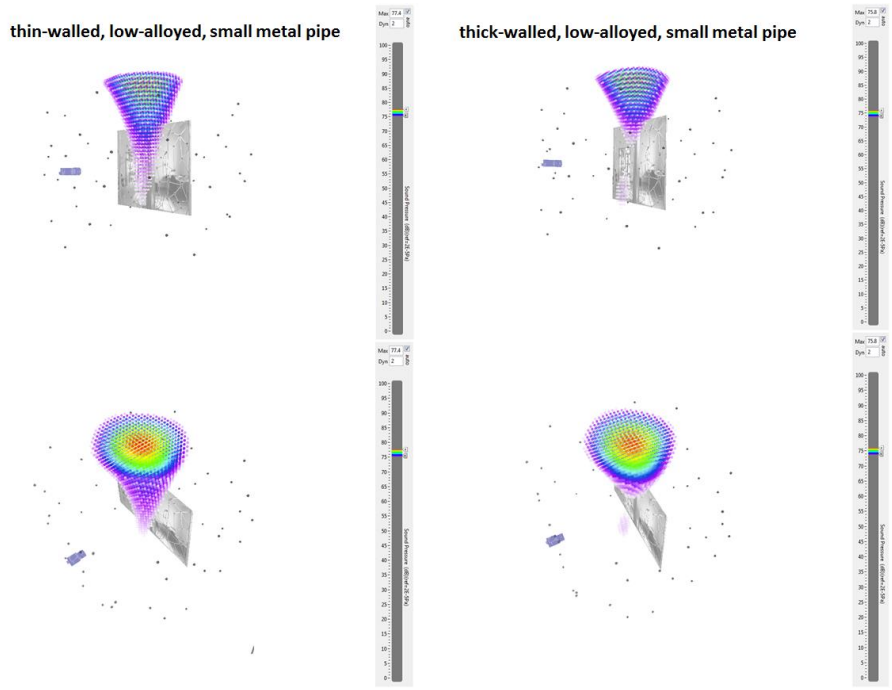

Figure 6: **Resulting colour-coded acoustic measurements on thin- and thick-walled, low alloyed small metal pipes.**

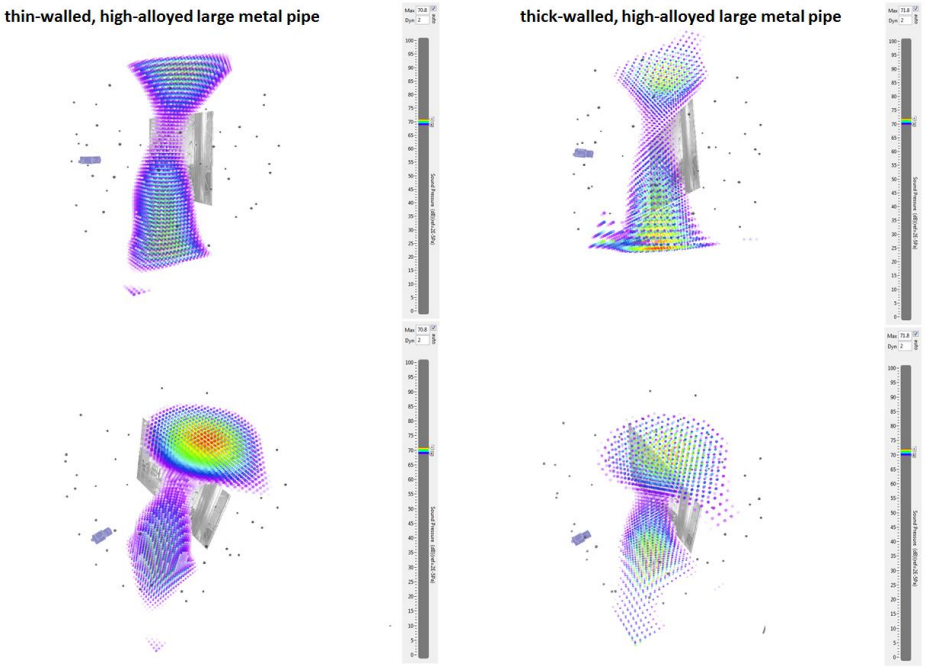

Figure 7: **Resulting colour-coded acoustic measurements on thin- and thick-walled, high alloyed large metal pipes.**

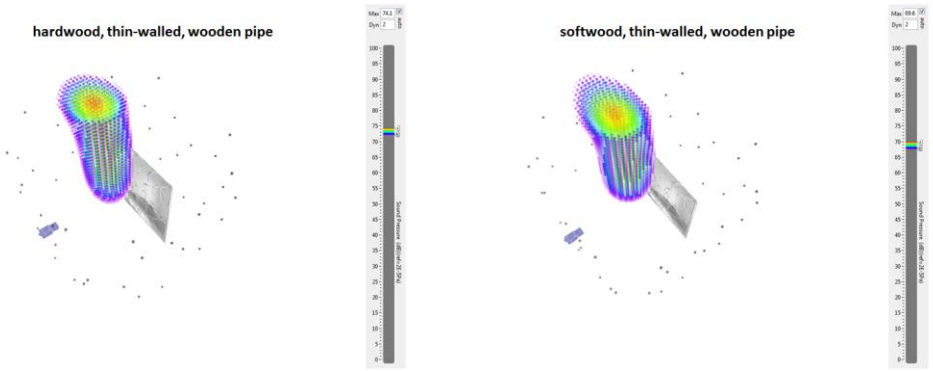

Figure 8: **Resulting colour-coded acoustic measurements on thin-walled, hardwood and softwood pipes.**

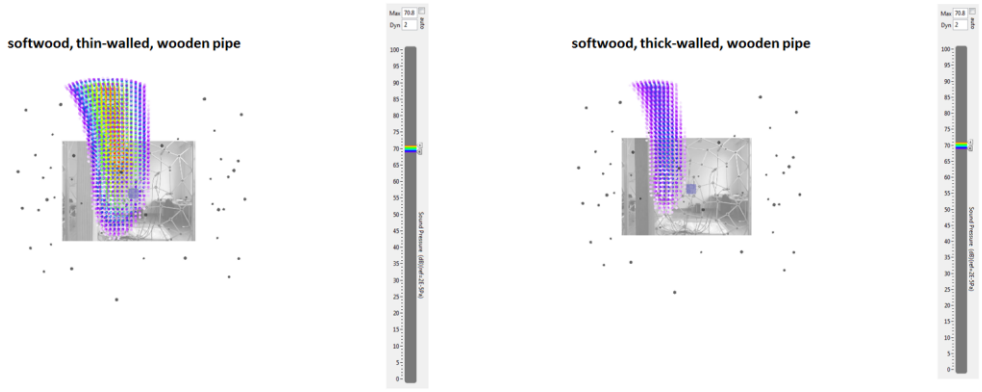

Figure 9: **Resulting colour-coded acoustic measurements on thin- and thick-walled, softwood pipes.**

Conclusions

The results of the organ pipe measurements generally show reasonable results relating to the sound level, which increases gradually from the outer walls to the centre of the pipes (Figure 6 - Figure 9), where the most motion of air particles takes place and hence, the maximum sound radiation occurs (red-coded). On the other hand, the results demonstrate crucial differences between the colour-coded development of sound diffusion at the top opening and the labium at equal frequency settings, Figure 6. This leads back to the individual design and material of the pipes. The sound radiation's behaviour of the metal organ pipes shows two opposing conical shapes meeting at the vertex (at the labium of the pipe, Figure 7), where less radiation occurs, while it shows an almost cylindrical behaviour in the case of wooden pipes (Figure 8, Figure 9). The colour-coded results demonstrate different sound intensities at different wall thicknesses, as thick walls offer lower sound radiation than thin walls, Figure 9. The thickness of the wooden organ pipes and different alloying of the metal pipes do not play a major role in the behaviour of the sound emission distribution on the pipes. The good quality of an organ pipe and the realisation of the player's own idea of an ideal sound might explain the fact, that different musicians prefer organ pipes with different materials.

- Acoustic measurements of a piano soundboard

Experimental details

The acoustic measurements on the soundboard of a piano were applied with the help of a camera that is mounted on a handheld intensity probes array by means of the acoustic near field holography method. The experimental setup of the measurement is shown in Figure 10.

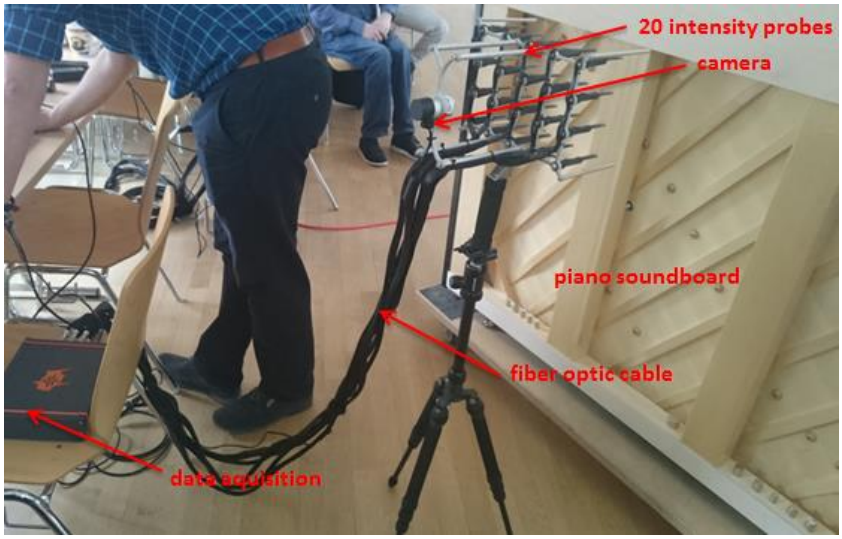

Figure 10: **Experimental setup of the acoustic measurements on the piano soundboard using a handheld intensity array.**

The measuring system is able to locate low frequency-stationary and -transient sounds starting from 40 Hz. The localisation took place by scanning predefined sections of the surface of the piano soundboard. The measured sections were selected by the piano maker, who developed a method to achieve more homogeneous tones out of the pianos with the help of positioning specific metal weight blocks (REE©)[1] on the selected sections. The displayed results on the PC using an associated software show colour-coded intensities at each probe position in a photo or a video. In contrast to the aforementioned acoustic 3D microphone array the live measurement of the handheld mobile array is the more favourable for the evaluation of sound. The soundboard was imaginarily divided into 9 sections (3 x 3 equal rectangles), where the final measurements were mainly applied in the upper right rectangle. The measurements took place in the frequency ranges of: 155 Hz - 235 Hz, 174 Hz - 176 Hz and 435 Hz - 445 Hz. The sound intensity data were transferred to the computer with the help of a data acquisition system of 24 bit and sampling rate of 48 kS/s.

Results and discussion

Figure 11 demonstrates one of the resulting colour-coded acoustic measurements on the upper right section of the piano soundboard, showing the sound intensity

[1] www.ree-verfahren.de/das-ree-verfahren, access: January 2016

behaviours in the cases of the application or of non-application of the REE© at a frequency range of 174 - 176 Hz. The measurements with REE© definitely constitute a difference in the sound intensity distribution on the selected sections of the piano soundboard. The distinct homogeneity of sound could be assigned to the smooth transition from lower intensity to higher intensity sounds, which could be established from the colour-coded results.

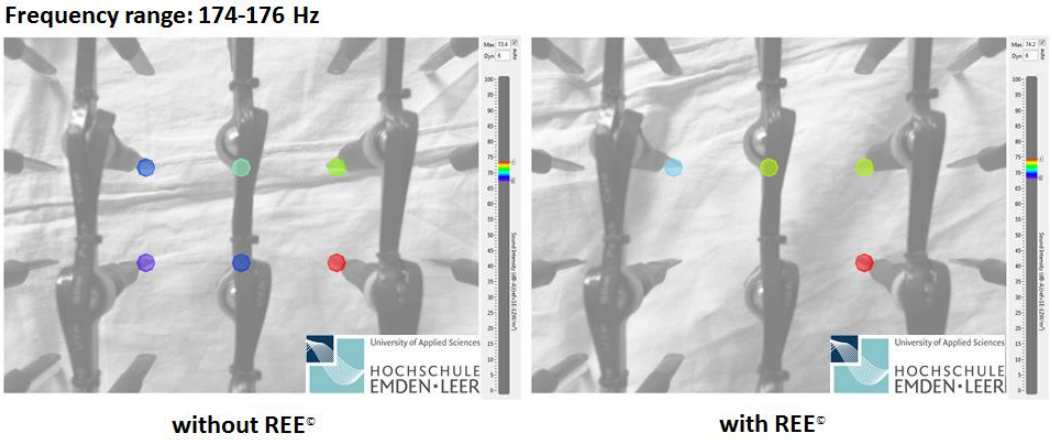

Figure 11: **Resulting colour-coded acoustic measurements on the upper right section of the piano soundboard using an intensity microphone array. Frequency range of 174 – 176 Hz.**

Conclusions

The experiment of the piano tuning presents a plausible possibility to locate the proper position of the metal weights. It is obvious that they create a more homogeneous or even harmonic sound as they, according to the resulting colour-coded live video and picture results, enable a smooth transition from lower to higher sound pressure level.

3. Acoustic measurements on board MS "Ostfriesland"

The passengers' comfort in transport vehicles like ships is degraded as long as structure-borne noise reaches a sound level that disturbs human wellness. The frequencies produced on vessels are dependent on several factors. These factors are the ship´s speed, the structure and the manufacturing material of the ship´s hull as well as the external voyage conditions (e.g. weather, tide, state of the sea), but most important is the propulsion. Acoustic measurements with common microphones are much less significant to big, slow operating main engines that lead to quite low oscillation frequencies on board. The Germanischer Lloyd (GL) defines vibration on board as "Structural oscillations in the frequency range of 1 to 80 Hz"[2]. With the help of special measuring instruments, it was possible to perform sound localisation measurements on board of the passenger vessel MS "Ostfriesland" within the framework of the research

[2] Germanischer Lloyd Aktiengesellschaft. 2009. Rules for classification and construction. I Ship technology: ch. 23, p. 1.

project MariTIM (project „MariTIM“; INTERREG IV A-Programme (http://www.maritim-de-nl.eu)) “LNG Passenger Vessel”. Subsequently, a reconstruction of the vessel was performed to test the technical and economic feasibility of an LNG electric propulsion system in passenger ships. Further acoustic measurements were performed after the ship’s reconstruction to investigate possible variations in the sound level values and sound intensity distribution in the passenger decks and in the engine room. The performed measurements after the reconstruction were evaluated and compared to the previous measurements before the reconstruction [9].

Experimental details

In order to visualise the sound field and to accomplish an accurate localisation of the sound pressure amplitudes occurring in different areas on the ship which are exposed to vibration, a sound source localisation system (acoustic camera)[3]. The system consists of a spiral microphone array with integrated digital camera, a data acquisition system and PC to process the data. The incident sound on the microphones is recorded synchronously, where the position and strength of the sound sources are determined and shown colour-coded. The main intention of the output data analysis was the detection of sound sources of constant frequencies, which provide information about the ship's acoustics. Due to the constancy of the frequencies over the entire measurement, the output data could be clearly assigned to the vessel, and not to other secondary effects, e.g. talking passengers. Further measurements with a sound level meter were synchronously performed to provide, with resulting absolute sound level values, a reference measurement to the colour-coded measurements of the acoustic camera. Due to shortage of space and possible loss of acoustic information in narrow corners inside the engine room, the measurements were carried out there with the help of a highly sensitive acoustic probe (Microflown™ probe, Microflown Technologies, NL), which was supplied with a digital camera that provided a correlated picture to the colour-coded measurements of sound pressure (for further use of this acoustic probe see also chapter 1: “Investigation of strain dependent damping of the titanium alloy Ti-10V-2Fe-3Al at room temperature”.) The following figure demonstrates the positions on the vessel, which were acoustically measured on the reconstructed vessel with the help of the mentioned devices.

[3] Prof. Dr. Jürgen Göken gratefully acknowledges the financial support of the German Research Foundation (DFG, www.dfg.de; DFG-reference number: INST 21572/1-1 LAGG).

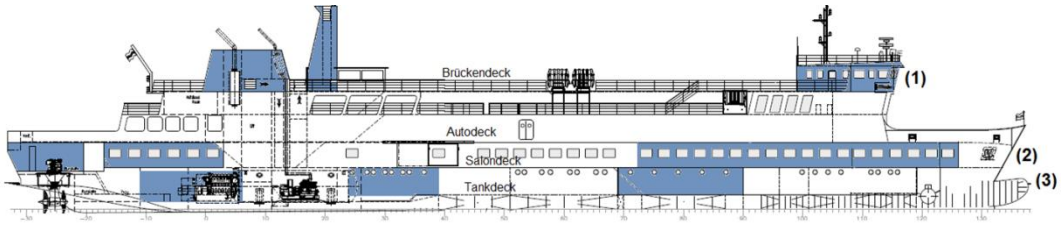

Figure 12: Acoustically measured areas on board of the MS "Ostfriesland"[4].

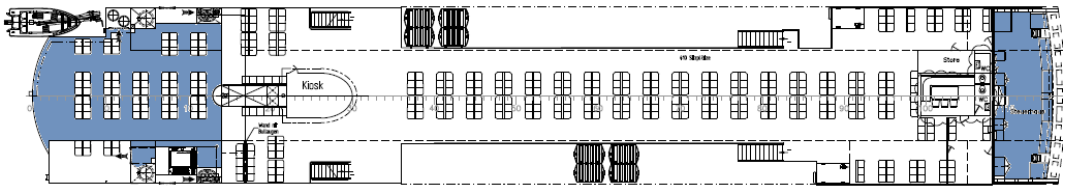

Figure 13: Bridge deck (1)[4].

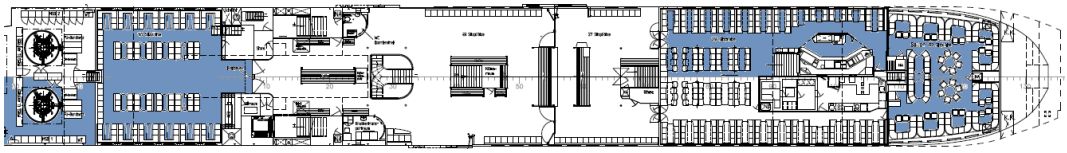

Figure 14: Saloon deck (2)[4].

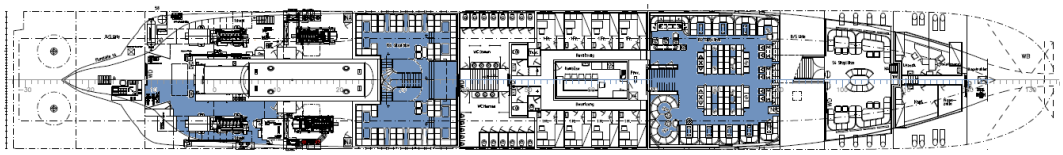

Figure 15: Tank deck (3)[4].

In the following section, an example of the measurements resulting from the spiral microphone array and another example of the measurements using the Microflown™ probe in the engine room are shown.

Results and discussion

Besides the importance of each of the colour-coded acoustic measurement results, using the spiral microphone array in each room on board, for the evaluation of the current ship acoustics a comparison between the situation before and after the reconstruction was of high interest. In order to ensure a direct comparison of the ship acoustics before and after the reconstruction, the same measuring conditions have to be met. This was only possible on board the "Ostfriesland" on the saloon deck in the aft saloon. There were no present passengers during the measurements neither before nor after the reconstruction, which allowed a direct comparison measurement in that room. An example of the comparison measurements is shown in Figure 16. The measurements after the conversion were evaluated with a software update, which leads to differences in the representation. It must also be considered that the saloon in its old form no longer exists and has been completely rebuilt and redesigned.

[4] AG „Ems“ (2013), www.ag-ems.de

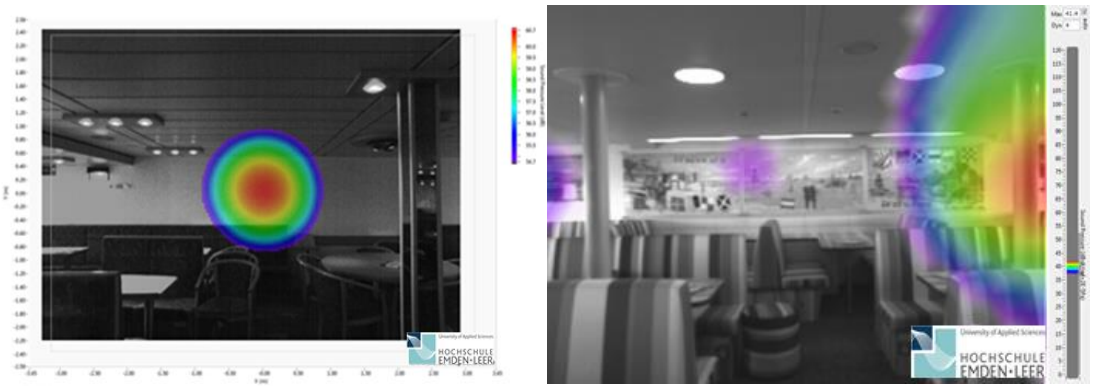

Figure 16: **Colour-coded acoustic measurement in the rear saloon before (left) and after (right) the reconstruction of the vessel. Frequency range: 1500 Hz - 1750 Hz.**

Before the reconstruction, a punctual sound source of 60.7 dB(A) was located at the rear wall at a measurement range of 1500 Hz and 1750 Hz. In the same frequency range, the new measurement shows a sound source at 41.4 dB(A) on the right edge of the resulting picture and no longer on the rear wall. The depicted right column was not yet available before the ship's reconstruction, which significantly changes the acoustics of the room. Further measurements within the frequency range of 4750 Hz - 5000 Hz show that the punctual sound source of 54.3 dB(A) is still visible at the rear wall before the reconstruction. The new measurement also exhibit a sound source at the same frequency range on the rear wall, as well as a further, more intense sound source at a table with max. 24.8 dB(A) in the left edge of the resulting picture. Likewise, smaller sound sources can be seen on the ceiling (partially through possible reflection) and on the left column. The performed measurements show that the ship acoustics in this room have been significantly improved by 19.3 dB(A).

The colour-coded measurements that were performed with the help of the Microflown™ probe in the engine/rudder engine rooms are described in detail in Ref. [9]. An example (measurement 1) is constituted in Figure 18. The accurate positions of this and further measurements are shown in Figure 17.

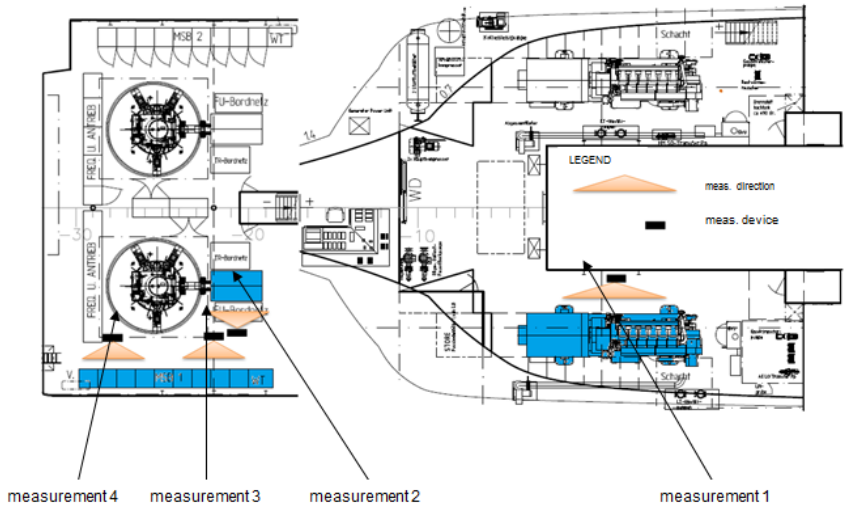

Figure 17: **Measuring points in the engine and in the rudder engine room (Microflown™ probe).**

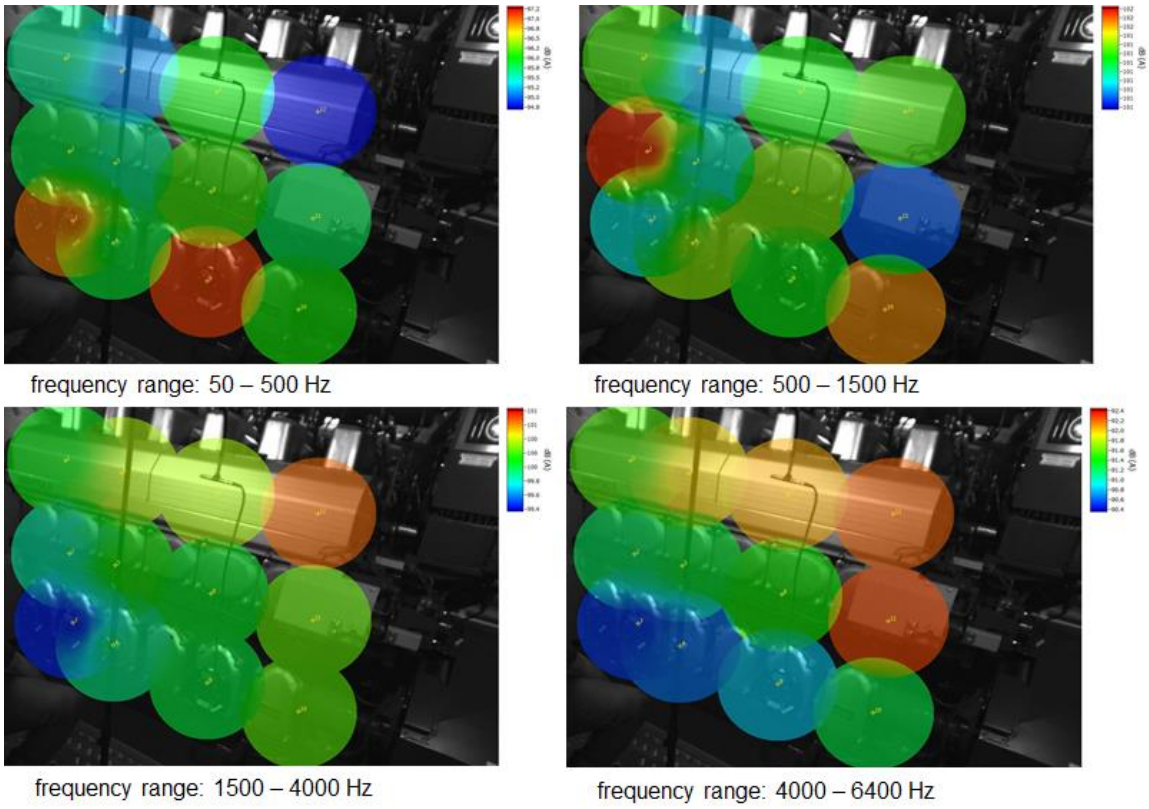

Figure 18: **Colour-coded measurement results (measurement 1, see Figure 17). Measurements performed with the help of the Microflown™ probe in the engine/rudder engine rooms.**

Conclusions

The investigations reveal that the extension of the ship, the redesign of the aft ship and the complete interior has practically developed a new ship from the vessel built in 1985. There are differences in maneuverability, loading capacity and drive performance. The powerful dual-fuel engines now operate at higher speeds than their predecessors. This has changed the ship's acoustics of the vessel especially in the engine room.

The measurements with the acoustic camera with spiral array, the Microflown™ probe and the sound level meter have reproduced the ship's acoustics under the current conditions. These conditions mainly include the present passengers on the crossings, which had a great influence on the results of the test. Nevertheless, in many areas of the ship constant frequency sound sources could be clearly located and assigned to the ship.

In order to be able to apply an accurate comparison, the same conditions inside the rooms must be met. This turned out to be extremely difficult, since except for a few exceptions, large structural changes took place in most of the ship’s sections, or the ship saloons have been completely renovated. Therefore, besides the huge useful processed data from the different applied measurements, a limited direct comparison could be performed. After extensive evaluation, the latest measurements were successful, since they prove that the reconstruction of the MS "Ostfriesland" has led to considerable changes in ship acoustics.

4. Studying the correlation between moisture content and damping properties of spruce wood

Wood is an inhomogeneous, anisotropic, porous and hygroscopic material of biological origin [10]. It is a natural construction material that has many advantages over other materials: High strength with good elasticity, high resistance against high load levels, corrosion resistance in saline water, good workability, low costs and its outstanding environmental friendliness [11]. One of the most important tone woods is spruce because of its good resonance properties; therefore it is widely used in the musical-instrument making, for examples for building sound boards that are the primary sound sources in pianos. However, the fluctuation of the moisture content in the wood affects the tone. With changing moisture content the instrument can go out of tune and at very low moisture content even cracks can appear in the wood. In addition the timbre will change. This can result from changes in the hammer felt, or in the changed vibration properties of the soundboard. Strain- and frequency-dependent damping measurements on spruce wood were carried out at different wood moisture content with the help of dynamic mechanical analysis (DMA), in order to investigate the moisture effect on the vibration behaviour. Preferably, wood slowly dried in air for several years is used for high-class pianos. Therefore, damping measurements on new and more than 130-year old spruce wood samples were performed. This report section concerns current investigations where further analysis of the results is performed to achieve the final assessment.

Experimental details

For this investigation, different aged spruce samples with the dimensions of about 80 x 10 x 1 mm^3 have been used. The moisture content of the samples has been primarily raised by subjecting two samples of the same type to steam for one hour until they reach a moisture content (MC) of about 45 %. One of those samples was left to dry in the air at room temperature, while its decreasing moisture content had been continuously measured at 30 seconds intervals with the help of a wood moisture meter with an accuracy of approximately ± 1 % in the moisture range from 8 % to about 40 %. The other moist sample was clamped in a dual cantilever sample holder, in which the sample is clamped at both ends and in the middle where it is subjected to bending load. The sample holder is mounted in the dynamic mechanical analyser EPLEXOR® 500N[5]. DMA machines work under the concept of applying a force to a material and analysing the material's response to that force (a non-resonance method). The force used in this case is sinusoidal and can be oscillated at a range of frequencies, typically 0.1 Hz - 200 Hz, and across a range of temperatures, typically -150 °C – 600 °C. From analysing this response, the DMA can calculate various properties from the recorded dynamic modulus E^* [12]. Cantilever fixtures are similar to 3-point

[5] Prof. Dr. Jürgen Göken gratefully acknowledges the financial support of the German Research Foundation (DFG, www.dfg.de; DFG-reference number: INST 21572/5-1 FUGG).

bending fixtures except that the ends and the middle of a sample are clamped. This introduces a shearing component to the distortion and increases the stress required for a set displacement. Therefore, the specimen must be loaded with the clamps perpendicular to the long axis of the sample and in addition, care must be taken to clamp the specimen evenly, with similar forces, and to not introduce a twisting or distortion in clamping [13]. A schematic layout of the dynamic mechanical analyser is shown in Figure 19.

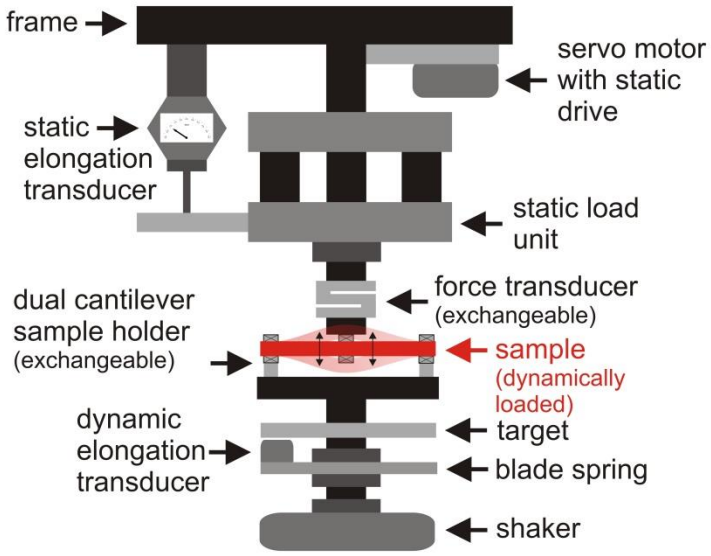

Figure 19: **Schematic layout of the dynamic mechanical analyser (DMA, EPLEXOR® 500 N), based on Ref.** [14].

7 successive measurements had been first applied on dry old and new spruce (moisture content ~ 8 %). These measurements included 5 strain-dependent measurements (dynamic sweeps) at frequencies of 12, 22, 33, 35, and 75 Hz respectively, then a frequency-dependent measurement (frequency sweep) at a dynamic strain of 50 % of sample height, and subsequently, a repetition of the first dynamic sweep at 12 Hz. A total of 162 successive measurements were applied on each of the moist spruce samples (new and old spruce). This included 27 measurement sets that started automatically after each other, where each set involved 5 strain-dependent and 1 frequency-dependent measurements. The strain-dependent measurements were carried out within a range of 0.3 to 50 % dynamic strain with an increment of 0.5 %, dynamic load of 499 N, static load of 1 N, and a contact force of 1 N. The frequency-dependent measurements were carried out within a range of 0.3 to about 70 Hz with an increment of 10 Hz, a static load of 1 N (maximum strain: 1 % of sample height), a dynamic load of 499 N (maximum strain: 50 % of height), and a contact force of 1 N. The moisture content of the clamped sample dropped gradually from approx. 45 % to reach a moisture content of approx. 10.9 % and 10.4 % at the end of the measurements series on new and old spruce, respectively.

Results and discussion

The dropping moisture content values that had been simultaneously measured on reference old and new spruce (Figure 20) and were analysed using a self-written LabVIEW™ program. The derivative curves of the raw data moisture content (in %) vs. time (in sec) curves were calculated, and the resulting curves were smoothed using moving averaging, Figure 21. These curves were determined for the investigation of the different rate of changes of the moisture content in old and new spruce. This was followed by a consecutive study of the water distribution behaviour inside old and new spruce wood with the help of microscopic analysis. After applying predefined constraints, the derivative curves (velocity of moisture change) were conditioned, to be used for the specific definition of different phases of considerable rates of change of moisture content. A corresponding DMA measurement set had been defined for each of those phases, and was investigated.

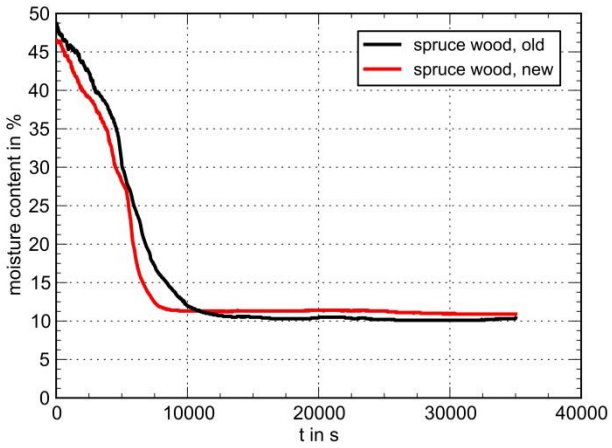

Figure 20: **Drying curves of old and new spruce wood.**

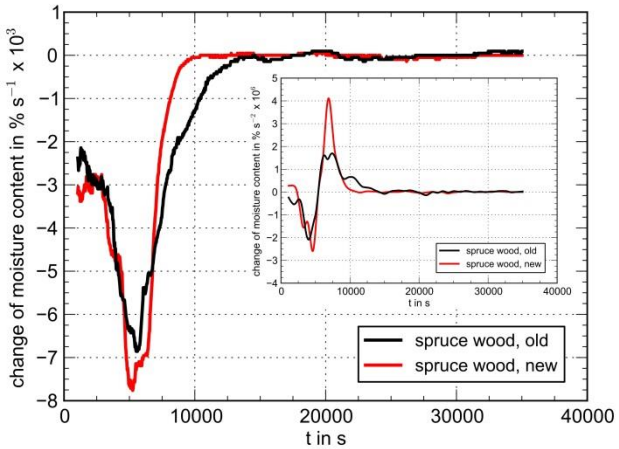

Figure 21: **Drying velocity curves of old and new spruce wood; inserted figure: Smoothed drying acceleration curves.**

The following figures present four examples of the resulting plots from the DMA measurements. The plots in Figure 22 show the relationship between the material damping which is represented by the loss factor *tan δ* and the strain *ε* (% of sample height; denoted here as deflection strain) in case of old and new spruce. The plots in

Figure 23 demonstrate the relationship between *tan δ* and the frequency (in Hz) of the sinusoidal signal of the applied dynamic force for both kinds of spruce in as-received state. The greater the time shift *Δt* between the signal force and sample distortion, the greater the loss factor *tan δ* and the loss modulus E´´ in the result.

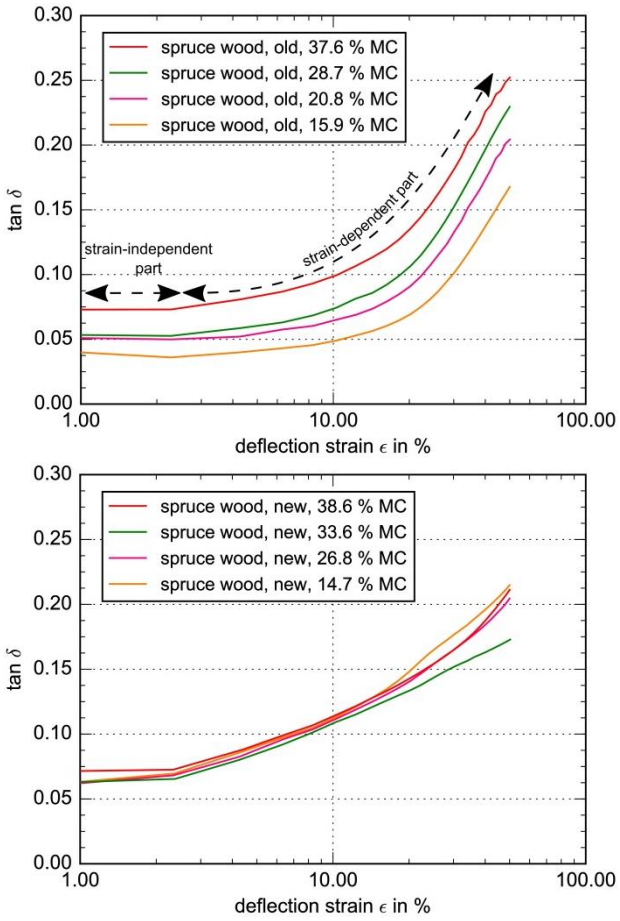

Figure 22: **Strain-dependent damping curves of old spruce wood (upper figure) and new spruce (lower figure) at a constant frequency of 12 Hz and variable wood moisture content (MC).**

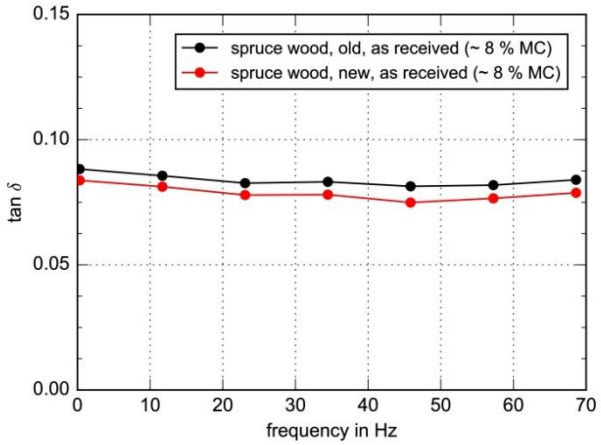

Figure 23: **Frequency-dependent damping curves of old and new spruce wood at a moisture content of nearly 8 % and a deflection strain *ε* of 50 % of the specimen thickness.**

Current conclusions

The drying curves of 130-years old and new spruce wood were different. Furthermore, the rate of moisture release (velocity of moisture change) were different, too, from which it may be assumed that the drying mechanisms of both woods are diverse. Damping measurements on old and new spruce wood showed that the material damping which was indicated in terms of the loss factor $tan\ \delta$ was almost frequency-independent over a frequency range of 0.3 to about 70 Hz but revealed a significant dependence on the strain. The measuring curves could be divided into a strain-independent and a strain-dependent part which is well known for metals when dislocation segments break away from pinning points. In contrast to the frequency, the moisture content had a significant influence on the damping behaviour of the old spruce wood. This may be attributed to the wood structure containing chemically degraded biopolymers. Further investigations are necessary to understand the correlation between wood moisture and the damping behaviour of the different aged spruce woods.

REFERENCES

[1] G. Srinivasu, Y. Natraj, A. Bhattacharjee, T. Nady and G. Nageswara Rao, *Mater. Des.*, no. 47, p. 323, 2013.

[2] M. Jackson, N. Jones, D. Dye and R. Dashwood, *Mater. Sci. Eng. A*, no. 501, p. 248, 2009.

[3] J. Göken, S. Fayed and P. Skubisz, *Acta. Phys. Pol. A, vol. 130,* p. 1352, 2016.

[4] W. Riehemann, Metallic Materials with Extreme Internal Friction and their Measurement, Clausthal-Zellerfeld: Papierflieger Verlag, 1996.

[5] J. Göken and W. Riehemann, *Mater. Sci. Eng. A*, no. 127, p. 324, 2002.

[6] J. S. Koehler, in *Imperfections in nearly perfect cystals*, New York, Wiley, 1952, pp. 197-216.

[7] A. V. Granato and K. Lücke, *J. Appl. Phys.*, vol. 27, no. 6, p. 583, 1956.

[8] P. Bleasdale and D. Bacon, in *Proceedings of the Third European Conf., Ed. C.C. Smith*, Oxford, Pergamon Press, 1980, p. 173.

[9] R. Eckert, Acoustic measurements on board M/V "Ostfriesland" (bachelor thesis), University of applied Sciences Emden/Leer, Faculty of Maritime

Studies: Leer, Germany, 2017.

[10] N. Okoye, A. Eboatu, R. Arinze, N. Umedum and O. P.I. Udeozo, *IOSR-JAC*, vol. 7, no. 6, p. 76, 2014.

[11] R. Falk, "General Technical Report FPL-GTR-190," in *Wood Handbook - Wood as an Engineering Material (chapter 1)*, Madison, WI, USA, 2010.

[12] A. Rasa, in *Proc. of the 43rd International Congress and Exposition on Noise Control Engineering - Improving the World through Noise Control (Internoise 2014)*, Melbourne, Australia, 2014, p. 4278.

[13] K. P. Menard, Dynamic mechanical analysis: a practical introduction, U.S.A: CRC Press, Taylor & Francis Group, 2008.

[14] "Netzsch Gabo Instruments GmbH," [Online]. Available: http://www.gabo.com. [Accessed 29 December 2016].

ISBN 978-3-944262-13-0